Effect of the monostearate/monopalmitate ratio on oral release of active agents from monoacylglycerols organogels

F. R. Lupi[1], V. Mancina[1], N. Baldino[1], O.I. Parisi[2], L. Scrivano[2], D. Gabriele[1]

[1] Department of Information, Modelling, Electronics and System Engineering, (D.I.M.E.S.) University of Calabria, Via P. Bucci, Cubo 39C, I-87036 Rende (CS), Italy

francesca.lupi@unical.it; mancina.valentina@gmail.com; noemi.baldino@unical.it; domenico.gabriele@unical.it; ortensiailaria.parisi@unical.it; luca.scrivano@unical.it

[2] Department of Pharmacy, Health and Nutritional Sciences, University of Calabria, Edificio Polifunzionale, I-87036 Rende (CS), Italy

Corresponding author

Dr. Domenico Gabriele

Department of Information, Modelling, Electronics and System Engineering (D.I.M.E.S.)

Via P. Bucci – Cubo 39C

I-87036 Arcavacata di Rende (CS), Italy

Email: domenico.gabriele@unical.it

22 Tel. +39 0984 496687; Fax +39 0984 494009

DOI: 10.1039/c8fo00594j

ABSTRACT

Delivery of active agents from organogels is becoming an important topic owing to the possibility of releasing, in a controlled way, lipophilic agents. Controlled release from foods is a topic with increasing relevance owing to the growing industrial interest towards functional or medical foods, i.e. foods containing nutraceutical agents or drugs. Anyway, release properties are related to the rheological properties of organogels, and, therefore, a deep knowledge of their microstructure and physical characteristics is necessary to design carriers with expected release properties. In this work, two low molecular weight gelators (i.e. glycerol monopalmitate, GMP, and glycerol monostearate, GMS) have been investigated using rheology, microscopy and infrared spectroscopy, IR, aiming at understanding the effects of different gelator ratios on organogel properties. It was observed that GMP, within the range of investigated compositions, seems to be more effective in yielding consistent organogels and this effect was related to differences in microstructure with respect to GMS. Their ability to control oral release of active agents was investigated, *in vitro*, using a chemoterapeutic drug for adenocarcinoma of the gastrointestinal tract, 5 fluorouracil (5-FU). A physical model based on carrier erosion was used to describe the release data, evidencing a good agreement with experimental values. Among the tested samples it seems that the use of 90% of GMS (over total organogelator content) yields promising results allowing a good partition of the released drug between the gastric and intestinal tracts with the largest value (although lower than 40% of loaded amount) of the total released drug.

Keywords: *organogel; oleogel; MAGs; glycerol monostearate; glycerol monopalmitate; 5 FU; controlled release*

1. INTRODUCTION

In the last few years, the interest in organogels (or oleogels), used alone or mixed to hydrogels for producing bigels as matrices for controlling delivery of active agents, has been increasing as confirmed by the number of recent papers or reviews focusing on this topic [1-6]. Oleogels are soft solids based on an organic solvent (an oil) structured by a network of organogelators that can be classified mainly in two groups, according to their molecular weight[7]: polymeric (PO) or Low Molecular Weight (LMW) gelators.

In food applications, the former are not so common and currently only ethyl cellulose is widely investigated in the literature[8]; on the other hand, food grade LMW gelators, such as alkanes and waxes, fatty acids and fatty alcohols, monoglycerides, phytosterols and others[8, 9], are more diffused; they can act through different gelation mechanisms like fatty acids crystallization, self-assembled fibrillary network, reverse spherical micelles[9].

In the recent past, the most investigated uses of these materials were addressed to the food industry[9], with the main purpose of substituting saturated fats in shortenings or margarines with healthier components able to impart the same rheological characteristics to the food [10] or as stabilising systems in oil-based food suspensions [11]. Nevertheless, drug delivery (through both oral intake and transdermal topical use) is becoming a new and very promising alternative for these materials that, owing to their characteristics, could be suitable for the production of food matrices able to control the release and the gastrointestinal absorption of active agents (both nutraceuticals or pharmaceuticals). Many of them, in fact, are lipophilic, therefore they could be dispersed more easily in an oil based system that could improve also the release and the oral bioavailability [12]. It is worth noticing that there is a significant attention of

pharmaceutical and food industry to the design of food matrices having specific and desired properties. These systems should be able to improve the release and the bioavailability of lipophilic agents that could be either nutraceuticals, to be used in functional foods, or pharmaceuticals, to be used in the so-called "medical foods", i.e. foods containing a drug to treat a specific diseases [12]. Starting from these considerations, a further investigation on delivery properties of edible oleogels and their relation to macroscopic characteristics, such as rheological properties, can be important to improve the current knowledge on this topic with the aim of designing food matrices for functional or medical uses.

From a microstructural point of view, organogels can be described as a network of organogelator molecules that aggregate into crystals and in their clusters. This network is able to entrap the organic solvent within avoiding liquid phase separation (syneresis). In addition, the organogel network is also able to entrap other particles or, simply, to stabilise them preventing their motion, such as aqueous phase droplets (forming W/O emulsions such as margarines substitutes), active agents (medical or functional foods) or other gels or solid particles (gelled emulsions or bigels). To explain better this classification, a schematic representation of organogels and their potential applications is shown in Fig. 1

Among the different edible gelators investigated in the literature, monoacylglycerols (MAGs, also called monoglycerides of fatty acids) have a big market and they are among the most studied, even in the recent literature [13-16]. Commercial MAGs are often produced by transesterification of fatty acids with glycerol, or synthesized via glycerolysis of triacylglycerol with alkaline catalysts under a nitrogen gas atmosphere [17]. This category of additives is commonly appreciated for their aptitude in stabilising

93 emulsions or food systems in general [18], or as gelling agents of oil phases eventually
94 used, in turn, to produce biphasic gels. For example, McSweeney et al. [19] studied infant
95 formula emulsions evidencing the effect of two emulsifiers, lecithin and
96 monoglycerides, on their stability, whereas Davies et al. [20], investigated a protocol to
97 obtain oil-in-water emulsions produced with glycerol monooleate (GMO) as the
98 emulsifier. Recently, Rafanan and Rousseau [21] used GMO and polyglycerol
99 polyricinoleate for emulsifying and promoting crystallisation of fat phase in water-in-oil
100 emulsions, and, moreover, pure glycerol monostearate (GMS) or mixtures with fatty
101 alcohol were also used to stabilise the oil phase (organogels) of bigels (organogel-in-
102 hydrogel) [22, 23]. As far as pure organogels investigation is concerned, different papers
103 give detailed descriptions of the role of MAGs in edible oil structuration [24-32].

104 A number of papers available in the literature discuss the properties of materials
105 produced with pure GMS used alone or mixed with other additives as an oil phase
106 gelator [27, 33-35], whereas pure GMP is never used for producing gels but always in a
107 commercial mixture with GMS.

108 In fact, most of the commercial MAGs are a mixture of GMP and glycerol monostearate
109 (GMS) in different proportions and according to the ratio of GMP over GMS, the
110 characteristics of the resulting organogel can be different. Lopez-Martinez et al. [31]
111 investigated organogels based on both commercial monoglycerides (made of GMS
112 37.7% and GMP 54%) and analytical grade monoglycerides (GMS 93.51%) in
113 safflower oil and they evidenced that the commercial mixture yields organogels with
114 higher values of storage modulus and higher solid fat content and with improved ability
115 to retain oil with respect to the pure GMS. These results were also confirmed when

MAGs mixtures, with similar composition, were used in canola oil with and without ethylcellulose [36].

Apart from these works, a lack of knowledge is currently evident in the literature about the effect of the GMS/GMP ratio on the physical properties and microstructure of organogels and on their potential uses.

In this work, organogels based on an edible oil (olive oil) and structured with MAGs having a different GMP/GMS ratio were investigated for producing matrices for oral delivery of active agents. From this point of view, the rheological properties of an organogel matrix can optimise the control of the agent to be delivered in the right period of time (not too fast, and not even too delayed) [37-39]. The specific interest of the research is mainly focused on the release of lipophilic agents modelled both with *in vivo* or *in vitro* methods, paying particular attention to the release kinetics.

The investigated organogels were produced with different mixtures of GMP and GMS with the aim of tuning the rheological properties of matrices for controlling the drug release. 5 fluorouracil (5-FU), a well-known chemotherapeutic active agent for adenocarcinoma of the colon, rectum, breast, stomach, pancreas [40], was chosen as active molecule to be released, exploring the potential use of these matrix in medical foods. Nevertheless, it is worth noticing that this agent was used to represent a class of agents that have to be released in a controlled way in the gastro-intestinal tract. Investigation and data analysis were performed independently of the chemotherapeutic nature of the agent (for instance no investigation on drug activity was developed) with the aim of studying the relation between release properties and formulation (the GMP/GMS ratio).

138 The investigation was carried out with a rheological characterisation based on both
139 small amplitude oscillation and steady in-flow tests. Rheological properties with
140 temperature were also compared with microstructural investigation based on IR spectra
141 and a rheo-optical analysis for the visual inspection of crystals forming the network. A
142 number of samples was loaded with 5-FU and its delivery with time from matrices was
143 investigated with *in-vitro* tests, giving also an interpretation of the release mechanism
144 with a model able to take into account the matrix erosion with time during the
145 gastrointestinal transit.

146

147 **2. MATERIALS AND METHODS**

148 The rheological investigation of organogels was based on samples produced by keeping
149 constant the total amount of organogelators (MAGs), but varying the ratio of GMP over
150 GMS.

151 **2.1 Materials**

152 Organogels were produced with a virgin olive oil (De Santis, Italy) as the solvent. GMS
153 ($C_{21}H_{42}O_4$, ACEF, Italy) was used pure (OS100 in table 1), or combined with Myverol
154 18 04 K, a commercial mixture of GMP ($C_{19}H_{38}O_4$) and GMS (equal mass fraction)
155 supplied by Kerry Group (Ireland). Adopted ratios are reported in table 1 where
156 investigated samples and their ID are shown.

157 In vitro bioavailability tests were carried out with several solvents and chemicals,
158 among which: 5-Fluorouracil 99% (HPLC grade), α-amylase and pancreatin from pig
159 pancreas, dialysis tubing cellulose membrane (cut-off: 12-14 kDa), methanol, sodium

160 bicarbonate ($NaHCO_3$) (-40 to +140 mesh), pepsin from pig gastric mucosa, and sodium
161 azide (all supplied by Sigma-Aldrich, USA), hydrochloric acid (37%, Panreac, Italy),
162 phosphoric acid (85%), sodium dihydrogen phosphate ($NaH_2PO_4 \cdot H_2O$) and sodium
163 hydrogen phosphate (Na_2HPO_4) all supplied by Carlo Erba (Italy) and HPLC-grade
164 water (VWR Chemical, Italy).

165 **2.2 Methods**

166 Organogels (100 mg for each sample) were prepared with an equal total amount of
167 gelators, but varying the ratio of GMS and GMP according to the composition reported
168 in table 1. The amount of pure GMS added to Myverol was progressively increased in
169 each sample, obtaining the mass fractions reported in table 1. Only samples produced
170 with 70, 80 and 90% of GMS of total MAGs were also loaded with the active agent 5-
171 FU to investigate its release.

172 2.2.1 Organogels preparation

173 As already described in previous papers [27, 28], organogels were prepared by warming the
174 oil up to 70°C in a continuously stirred beaker (stirrer RW 20, IKA, Germany)
175 thermostated with a water bath (plate heater Jolly 2, Falc Instruments, Italy). When the
176 oil reached the desired temperature, the gelators were added allowing their complete
177 melting. After further 5 minutes of rest time (continuing to stir the liquid), samples were
178 directly loaded into the rheometer geometry, where optical and rheological tests were
179 carried out.

180 Samples for IR spectroscopy investigation were prepared following the procedure
181 already described. Then, melted organogels were stored at room temperature until the

gelation was completed; samples were stored at room temperature for one week and afterwards 0.02 g was loaded into the measurement chamber to be investigated.

As far as the organogels loaded with 5-FU are concerned, after the gelators addition, also 5-FU was added to the melted oil phase, since the temperatures reached were not so high as to damage it [41]. Afterwards, melted organogels were poured inside capsule-shaped moulds in order to obtain pills of approximately 0.7 grams each; afterwards, samples were allowed to cool down to room temperature. A control sample, labelled as 'FO', was produced adding 5-FU to pure liquid oil, in order to compare the release ability of the organogels to that of the corresponding unstructured sample. The ratio 5-FU/oil was kept constant and equal to 0.016.

2.2.2 Rheological and rheo-optical characterisation

Rheological characterisation of samples was carried out with both small amplitude oscillation tests (SAOTs) and steady shear tests. Dynamic temperature ramp tests (time cure) at 1 Hz and Step Rate Temperature Ramp Tests (SRTRTs) at 1 and 10 s^{-1} were performed with a strain controlled rheometer (ARES RFS, TA instruments, USA) equipped with a parallel plate geometry of ϕ=50mm, (gap=1±0.1 mm) with a Peltier system acting under the lower plate for the thermal control of the sample. Temperature was decreased from 70°C down to 10°C with a cooling rate of 1°C/min. Preliminary strain sweep tests at 1 Hz were carried out to determine the linear viscoelastic regime [29] over the whole investigated range of temperature.

Rheo-optical analysis was performed with a stress controlled rheometer HAAKE MARS III (Thermo Scientific, Germany) equipped with a RheoScope module (camera Foculus FO232TB monochrome, magnification of the lens 20X, Thermo Scientific,

205 Germany) for which a parallel plate geometry (polished plate, ϕ=60mm, gap=1±0.1
206 mm) and a Peltier system were adopted. Micrographs were taken manually at the
207 temperature values corresponding to noticeable changes detected in time cure tests.

208 Both SAOTs and SRTRTs were used to evaluate the onset of crystallisation temperature
209 *Tco* corresponding to the temperature at which a sudden increase of the complex
210 modulus or viscosity according to the test, and, contemporary, a strong decrease in
211 phase angle was encountered. The mathematical methods adopted for evaluating these
212 values are the same as already described by Lupi et al. [29, 30]. Moreover, gelation
213 temperature *Tg* has been assumed as the value corresponding to the crossover between
214 dynamic moduli, i.e. a phase angle of 45° [29].

215 In some cases, experimental data were compared among them with a statistical analysis
216 based on a *t-student* test (Microsoft Excel 2016, Microsoft Office, USA). Differences
217 among values were considered significant at *p-value* < 0.01 (interval of confidence of
218 99%). All data fitting was performed through Table Curve 2D Software (Jandel
219 Scientific, USA).

220 2.2.3 IR characterisation

221 IR absorption spectra of organogels and pure organogelators mixtures were collected at
222 room temperature (about 20°C) using a Nicolet iS-10 FT-IR spectrometer (Thermo
223 Scientific, USA) equipped with a Smart iTX ATR sampling accessory. Spectra were
224 detected within the range of wavenumber between 400 and 4000 cm^{-1} (data spacing
225 0.482 cm^{-1}, 64 scans for each test). Organogels were prepared as already discussed.
226 Curves analysis, including the calculation of peak intensity (i.e. the areas under the

peaks), if necessary, were carried out with the software Spectragryph 1.2.8 (Dr. Friedrich Menges Software-Entwicklung, Germany).

2.2.4 *In vitro* drug bioavailability and delivery tests

In vitro bioavailability tests were performed in simulated gastro-intestinal environment, employing the previously published protocol [38]. Samples for the experiments were prepared as follows: 5-FU-loaded organogels were obtained by putting the same amounts of drug in the organogelators/olive oil mixtures at 70°C (Table 1). Afterwards, they were poured in the moulds in order to obtain the final formulations. As control and as blank, a solution of 5-FU in olive oil and organogels without 5-FU were also prepared, respectively. The test is based on two enzymatic phases: pepsin digestion, which occurs in 2 h, and pancreatic digestion, which occurs in the following 4 h.

2.2.4.1 Pepsin digestion

The capsules containing 5-FU and prepared with different GMP/GMS ratios, blank capsule and 5-FU olive oil solution were put in different dialysis bags, each filled with 1 ml of 0.85 N HCl solution, 3 ml of 0.04% sodium azide (NaN_3) solution and 44 mg of porcine pepsin. The membranes were carefully sealed at each end and immersed in 20 ml 0.85 N HCl solution. Systems were incubated in a shaking water bath at 37 ± 0.5°C for 2 h, in order to simulate gastric digestion.

2.2.4.2 Pancreatic digestion

Following the gastric phase, the membranes were recovered, opened and 1.3 ml of 0.8 M $NaHCO_3$ solution, 11 mg of amylase and 11 mg of porcine Pancreatin were added to them. The dialysis bags were then sealed again and placed in 20 ml of phosphate buffer

249 saline (PBS) solution at pH 7.0. The samples were incubated again at 37 ± 0.5°C for
250 further 4 h.

251 *2.2.4.3 HPLC analysis*

252 At the end of the time points, volumes of the releasing media were analysed by HPLC.
253 The instrument is made up of a Jasco pump PU-2080 Plus and a Jasco UV detector
254 2075 Plus. A 250×4,60 mm CN column, packed with 5 μm particles (Phenomenex,
255 Torrance, CA, US) was employed, the mobile was made of water/methanol/phosphoric
256 acid (97.95/2/0.05) and the flow rate was 0.5 ml/min.

257 2.2.3 Total weight loss tests

258 Organogel capsules (unloaded samples OS70, OS80 and OS90) were placed in 5 ml
259 sintered glass filters (Ø10 mm; porosity, G3, i.e. 16-40 μm nominal maximum pore
260 size), weighed and immersed in 0.85 N HCl for 2 h and then in PBS solution at pH 7.0
261 for 4 h, in order to evaluate material weight loss in gastro-intestinal simulating fluids.
262 Every 30 min, the excess of water was removed first by percolation and then by
263 centrifugation for 5 min at 2000 rpm. Finally, the filters were weighed and organogel
264 masses were calculated by subtraction of the filter tare. Percentages of mass loss were
265 obtained using the following equation:

266 $$Mass\ loss\ (\%) = \frac{\left[\left(W_{tx} - W_f\right) - \left(W_{t0} - W_f\right)\right]}{\left(W_{t0} - W_f\right)} \times 100 \quad (1)$$

267 In which W_{tx}, W_f and W_{t0} represent the weight of filter with the organogel at different
268 time points, the weight of the empty filter and the weight of the filter with organogel at
269 0 h.

3. RESULTS AND DISCUSSION

3.1 Organogel-based capsules

The oral route of drugs administration is the most commonly used one due to several advantages, such as its simplicity and convenience, which result in an improved patient compliance. On the other hand, this way of administration present some limits including a variable bioavailability affected by several factors such as first-pass metabolism, acid stability and enzymatic degradation, the presence of food, gastric emptying time and intestinal motility, metabolism and transport.

5-Fluorouracil is one of the most important anticancer drugs. This antineoplastic agent is a nucleoside metabolic inhibitor used in the treatment of colon, rectum, breast, stomach and pancreas cancer but its efficacy could be limited by its pharmacokinetics. Recently, several clinical studies highlighted that chemotherapeutic regimens involving oral 5-FU drugs are not inferior compared to the continuous 5-FU infusion chemotherapy [42].

Based on these considerations, in the present research study, organogels for 5-FU delivery were prepared with the aim to develop organogel-based capsules for the oral administration of this therapeutic agent. This kind of dosage form, indeed, is characterized by different advantages including ease of handling and transport and high patient compliance. Organogels allow drugs to be delivered via a simple administration route, such as the oral one, enhancing the bioavailability and promoting the drug protection against degradation processes. Moreover, organogels-based capsules are

characterized by a high simplicity of production, flexible storage conditions and the possibility of using natural biodegradable starting materials; therefore, they can find a potential application for the oral administration of 5-FU improving its bioavailability.

3.2 Rheological characterisation of organogels

Organogels are known for their thermoreversibility, for their soft-solid consistency below *Tco*, and because their behaviour is a function of the quality and the quantity of organogelator added to the solvent, as well as of its chemical characteristics. Organogels studied in this work follow the described behaviour, and, as an example, Fig. 2 shows the time cure test in terms of G^* (Fig. 2a) and phase angle δ (Fig. 2b) of unloaded samples (OS50-OS100). Time cure tests reveal a liquid-like behaviour of systems (evidenced by phase angle values close to 90° starting from high temperatures down to Tco (Tco values of samples are listed in table 1; they were computed by both SAOTs and steady tests). Viscosity curves (which are shown in the supplementary material in figs. SM1 and SM2) retrace the qualitative behaviour of complex moduli, and the onset of crystallisation found in time cure tests corresponds to the same temperature values found for each samples in step rate tests at 1 s^{-1} (Table 1, $p>0.01$). If the shear rate is increased to 10 s^{-1}, the qualitative trend of viscosity as temperature function is the same as observed at 1 s^{-1}, but the estimated Tco becomes significantly different with respect to data at 1 s^{-1} (according to the *t-student* test) if the ratio X_{GMS}=GMS/MAGs is higher than 0.7. Figure 3 shows the value of ΔTco evaluated as

$$\Delta Tco = Tco_{1s^{-1}} - Tco_{10s^{-1}} \quad (2)$$

as a function of X_{GMS}. It is interesting to notice that the difference between Tco evaluated at the two values of shear rate according to the GMS content, and, in particular, it increases with the amount of GMS added to the system, up to an apparent plateau, evidenced at X_{GMS} higher than 0.7. These experimental evidences point out the higher "efficiency" of GMP in stabilising the organogel network with respect to GMS. In fact, when a fraction of GMP of at least 0.3 is present within the organogelator mixture, the crystallisation of samples is a unique function of the organogelator amount and it does not depend on the kinematics conditions adopted for carrying out the tests.

Some interesting considerations about sample rheology can be evaluated at a temperature value far below Tco, so that the crystalline network is completely formed, avoiding data analysis in the transition region [43]. Rheological parameters, G*, δ and η at both the investigated shear rate, were examined at T = 20°C, and the results are shown in Figure 4 in terms of viscosity (Fig. 4a) and G* and δ (Fig. 4b) as a function of X_{GMS}. Viscosity decreases monotonously increasing GMS and an apparent plateau can be noticed at X_{GMS}=0.8 for the lowest imposed shear rate; increasing further GMS content, viscosity values can be considered constant within the range described by the error bars. At 10 s^{-1} the downward trend reaches the constant value of viscosity at X_{GMS}=0.7. This difference is caused, probably, by the more intense shear action at 10 s^{-1} that hinders the network formation and yields an apparent plateau at a very low viscosity (close to 0.5 Pa·s).

When complex modulus (examined in linear condition, where, by definition, the sample is not damaged by the investigation technique) is considered, it can be seen that it decreases in a monotonous way if GMS increases and no plateau can be noticed in this case, supporting the hypothesis that the previously discussed viscosity plateau can be

338 attributed to shear action on the forming network. On the other hand, a different trend is
339 exhibited by the phase angle that seems to reach a maximum (equivalent to a minimum
340 degree of structuration) at $X_{GMS}\approx0.8$ suggesting a variation in organogel microstructure.
341 Apparently, more structured materials (i.e. with lower phase angle values) are obtained
342 when pure GMS or Myverol are used, whereas different ratios yields to less structured
343 systems.

344 In order to reassume the rheological results so far described, it can be concluded that the
345 variation of the ratio of GMS over GMP within a fixed mass fraction of monoglycerides
346 of fatty acids added to the oil has a strong influence on the final consistency and
347 thermorheological properties of organogels. In particular, at a temperature value lower
348 than the onset of crystallisation (i.e. 20°C), GMP seems to be more "efficient" than
349 GMS in imparting stiffness to the gel and, in fact, this result is highlighted by the trend
350 of G* with the mass fraction of GMS that decreases monotonously, whereas the phase
351 angle shows a maximum value at $X_{GMS}\approx0.8$, as already discussed. As far as the "in-
352 flow" results are concerned, they partly retrace what was already deduced from small
353 amplitude oscillation tests, showing a viscosity decrease in cold conditions when GMS
354 increases. Nevertheless, it has to be said that viscosity curves show a slope change
355 increasing the amount of GMS that varies with the adopted shear rate. Even the
356 thermorheological parameters T_{CO} and Tg are affected by the ratio between the two
357 monoglycerides: they both decrease when GMS increase, and T_{CO} calculated from
358 SAOTs is comparable just to the T_{CO} derived from SRTRT at $1s^{-1}$ i.e. the lowest
359 adopted shear rate, whereas increasing shear rate, these temperature are no longer
360 comparable. Thus, it is evident that the extra-ethyl group of GMS is able to weaken the
361 organogel matrix, owing to an increased steric encumbrance. Different ratios of

monoglycerides could be used in order to tune the final properties of the material according to their final use, in terms of consistency and thermal stability. For instance, in the particular case described in this paper, the matrix used for the active agent delivery should be consistent enough to avoid an immediate release of the molecule, but not too strong to delay its erosion preventing the release of the right amount of agent.

3.3 IR spectroscopy

IR spectroscopy is a valid tool to understand the intermolecular interactions that promote gel formation. According to the literature [44, 45], LMW organogelators are able to self-assemble creating the crystalline network thanks to the establishment of weak interactions such as H-bonds or van der Waals. In particular, it has been found that MAGs network formation in olive oil is principally promoted by H-bonds occurring between the –OH free groups in the glycerol molecule and the C=O groups of fatty acids [46] and a minor contribution is given by the van der Waals interactions standing between fatty acids tails [28]. In an IR spectrum of MAGs organogels, the most interesting wavenumber region is in the range 2500-4000 cm^{-1} where both kinds of interactions can be identified. Figure 5a shows IR spectra of samples at 20°C measured after 1 week of storage at room temperature. As also pointed out by the circle in the figure, the broad peaks corresponding to the wavenumber region between 3000 and 3500 cm^{-1} are representative of stretching modes of glycerol –OH groups [46].

Generally speaking, the shift of these prominent peaks towards lower energy regions with respect to a condition of unstructured (and, therefore, unlinked) samples, suggests the H-bond formation [47], which, obviously hinders the chain mobility. On the contrary,

384 the increase in peaks broadness can be attributed to the increase in the number of
385 vibrating -OH groups potentially creating bonds [48].

386 As shown by the enlargement of the region of interest shown in fig. 5a, peaks shape and
387 broadness changes considerably, passing from small inflections of the spectrum in
388 sample OS100 to a well-developed twin peak in sample OS50. Therefore, it can be
389 speculated that the increase in GMS fraction results in the reduction of peak area of the
390 corresponding organogel, and a lower propensity to give H-bonds as a consequence
391 (this could explain the rheological behaviour described). As a confirmation of this
392 experimental evidence, the peak intensities, i.e. the areas under the OH groups' peak
393 (A_{OH}) calculated in a wavenumber range between 3649 and 3049 cm^{-1} were evaluated,
394 applying an individual baseline for each curve. Fig. 5b shows the relation between *G'* of
395 each organogel with the corresponding area A_{OH}, highlighting a monotonous trend of the
396 rheological parameter with the number of vibrating OH groups, in turn responsible for
397 H-bonds formation. In previous works, a fractal nature of the organogels rheology as a
398 function of the organogelator content was already discussed [28, 43] and it was shown that
399 the storage modulus G' can be related to the solid fat fraction, Φ, by the so-called
400 "modified fractal model" [49]:

401 $$G' = \lambda\left(1 - e^{-k\Phi^b}\right)^{\frac{1}{3-D}} \quad (3)$$

402 In eq. 3, λ is a constant according to the strength of the interactions between crystal
403 aggregates; D is the fractal dimension of the system (for MAGs organogel a mean value
404 of 2.74 was obtained in previous works, see Lupi et al. [28]); k and b are constants linked
405 to the number of clusters within the fat [49].

406 It is worth noticing that, in organogel, the solid fraction corresponds to the
407 organogelator molecules that, interacting with each other, build the crystalline network.
408 As a consequence, it seems reasonable to assume that the solid fraction, Φ, is a function
409 of the interactions (in the present case only H bonding) among organogelator molecules
410 that, in turn, can be described by the area of OH groups peak in the IR spectra. Starting
411 from these considerations a further modification of the fractal model (Eq. 3) could be
412 proposed, introducing a dependence on the peak area A_{OH}:

413 $$G' = \lambda\left(1 - e^{-k' A_{OH}^{b'}}\right)^{\frac{1}{3-D}} \quad (4)$$

414 Experimental data were fitted with eq. 4, assuming D=2.74, and a very good agreement
415 of experimental data and fitting curve was observed (see Fig. 5b), obtaining λ=1330 Pa
416 ± 80 Pa, k'=0.022 ± 0.005 cm/% and b' = 0.719 ± 0.004.

417 If the pure organogelators spectra are considered, GMS usually shows a broad peak
418 with a small shoulder [27], whereas Myverol is characterised by a well developed twin
419 peak [28]. In the twin peak appearing in all the spectra, the higher wavenumber peak
420 corresponding to about 3309 cm^{-1} is the peak of the 3-OH group [46] whereas the other
421 one (at about 3237 cm^{-1}) is the peak given by the vibration mode of 2-OH. This last
422 group, according to Chen and Terentjev [46], dominates and eventually replaces the other
423 bonds completely in building the network. In fact, the authors suggest that with aging,
424 3-OH hydrogen bonding is not stable and tends to reduce, playing only a secondary role
425 in MAGs organogel structuration. This transition, during aging, corresponds to the
426 transition from a sub-α crystal phase to a more ordered β crystal phase [46].

About this, the ratio between the transmittance values of peaks 2-OH over 3-OH ($t_{2\text{-}OH/3\text{-}OH}$ in Fig. SM3 shown in the supplementary material) decreases with the increase of GMS fraction, even if the range is very narrow. Therefore, it is probable that the additional ethyl group, which distinguishes GMS from GMP, hinders group 2-OH, preventing it from forming an H-bond. This should further explain the higher consistency of the resulting organogel produced with the major content of GMP.

3.4 Rheo-optical analysis: photomicrographs

A rheo-optical analysis was carried out for both time cure and in-flow tests to evaluate the evolution of crystals in terms of shape and dimension during measurement. Fig. 6 shows the crystalline microstructure of samples OS50, OS70 and OS100 at 20°C obtained with time cure tests and with SRTRTs at both the adopted shear rate values. Going from sample OS50 (containing the minimum amount of GMS with respect to the other samples studied in this work) to OS100 (prepared with the maximum amount of GMS), the crystalline shape changes considerably: crystals are fibres of different dimensions for sample OS50, and in particular they appear slightly bigger in the case of SAOTs tests. In the latter case, the dimension of fibres do not seem to be affected dramatically by the increase in the shear rate value. Increasing the amount of GMS, crystals arrange into big spherical aggregates of plate-like crystals (as already observed by Hwang et al. [50] for sunflower wax crystals formed in an edible oil organogel) whereas a spherulite nature, evidenced by the Maltese cross [51], appears when GMS is the only organogelator. These crystalline arrangements could explain the rheological differences given by the use of GMS and GMP mixtures of gelator.

3.5 Release of 5-FU: a pharmaceutical application

Considering the results discussed about the rheological properties of organogels, it is clear that the most consistent samples were obtained with the highest amount of GMP added to the oil in the mixture of organogelators. These results led to some speculation for the selection of samples for 5-FU delivery by oral administration. Too consistent samples could ensnare the active agent reducing its availability, whereas samples with a low consistency could give a too fast a release of the active agent. Therefore, only 3 samples, with a GMS content varying from 70 to 90%, were chosen for the pharmaceutical experimentation. *In vitro* tests were divided into two subsequent steps simulating the transition of the material into the gastro-intestinal tract. The first step lasted 2 hours, the second, 4 hours, for a total duration of the experiment of 6 hours. Figure 7 shows the release of 5-FU, in terms of fraction released in each tract (the "gastric" and the "intestinal" tract), with respect to initial drug mass. In the gastric tract, a little amount (about 14.5% for the less structured sample) of the active agent is released by the organogels, whereas the pure unstructured oil releases 75.8% of the compound. In the subsequent simulated tract, the maximum amount of 5-FU (about 21.1%) is released by the most unstructured sample (FOS90) and, obviously, by pure oil. It is worth noticing that the proper release of the active agent should be balanced within the gastro-intestinal tract allowing the molecule to be properly delivered in the section of the lumen were it should exert the therapeutic activity [52]. Of course, pure oil does not control this release, concentrating the delivery of the active agent almost totally in the first two hours following the oral administration.

473 The release process, of active agents from a matrix, can occur according to different
474 mechanisms based either on diffusion of the drug through the matrix or on dissolution
475 of the carrier (or on the combination of both of them) [53, 54]. In the first case, the dosage
476 forms remain intact and the active agents diffuses within the matrix to the surface, then
477 it is transferred to the surrounding medium (through the interface) and, finally, it is
478 transported away from the surface[54]. In the second case, the carrier erodes releasing the
479 agent and changing the dimension (and the external surface) with time: erosion can be
480 heterogeneous (degradation occurs within a thin external layer) or homogenous
481 (degradation occurs throughout the polymer matrix)[54]. Erosion can occur in
482 combination with diffusion and the final release rate depends on both of them or on the
483 limiting mechanism.

484 Different models were prosed in the literature to describe the release rate and the
485 amount of released agents. One of the first models was proposed by Higuchi to describe
486 the diffusion mechanism; assuming that internal diffusion can be described by Fick's
487 law and using some simplifying hypothesis (see the work by Raza[53] for further details)
488 he obtained:

489 $$Q = A\sqrt{D\left(2C_0 - C_s\right)C_s t} = k_H t^{\frac{1}{2}} \quad (5)$$

490 where Q is the released drug in time t per unit area A, D is the diffusion coefficient, C_0
491 and C_s are the initial and the equilibrium concentration of agent, respectively, and k_H is
492 the Higuchi constant. Among the further different models proposed in the literature, the
493 empirical Korsmeyer-Peppas equation [55] has been widely used, with good results, to
494 describe drug delivery from polymeric systems[53] and also from organogels [38, 56]. This

model relates the cumulative fraction of released drug, *F(t)*, to process time, *t*, with a power law:

$$F(t) = k_1 t^n \quad (6)$$

where k_1 is the release rate constant (i.e. a specific release rate) and *n* is the release exponent. According to the literature, [38, 57], if the matrix into which the molecule is entrapped is spherical, if *n* is lower than 0.43 the diffusion release can be considered as Fickian, for $0.43 \leq n \leq 0.85$ an "anomalous" non-Fickian mechanism is present, and, finally for $n \geq 0.85$, the transport is of the type case II, involving matrix dissolution; when n=1 the release follows a zero order kinetic corresponding to a constant release rate[53]. Therefore, this model seems able to describe the effects of different release mechanisms.

When erosion is the controlling mechanism a mathematical model was developed by Hopfenberg to describe the released rate from a matrix assuming that surface area remains constant during degradation process[53, 54]:

$$\frac{M_d(t)}{M_{d\infty}} = 1 - \left[1 - \frac{k_0 t}{C_0 r}\right]^n \quad (7)$$

where $M_d(t)$ is the drug mass within the carrier at each time *t*, $M_{d\infty}$ the total amount of active agents that can be released (in infinite time), C_0 is the initial agent concentration within the carrier, k_0 is the erosion constant, *r* is the initial characteristic dimension of the carrier (radius for cylinder and sphere, length for a slab) and *n* an exponent dependent on the geometry (n=1 for slab, 2 for cylinder, 3 for sphere). Further different

515 models proposed to describe the release rate from different systems (based on erosion
516 and /or diffusion) are described more in detail by Pothakamury et al.[54] , Raza et al.[53].

517 Even if delivery from organogel is becoming an interesting topic, so far specific release
518 models for these materials do not exist, according to the literature it seems that matrix
519 erosion or erosion-diffusion phenomena can be the most important mechanisms and the
520 Korsmeyer-Peppas equation (Eq. 6) has been used with positive results[38, 56].

521 Nevertheless, a different approach could be proposed based on the investigation and
522 modelling of erosion phenomena; starting from these considerations, in order to better
523 investigate the mechanism of release from the organogelled matrix, the erosion profile
524 of carriers was investigated monitoring the total volume loss from samples within 6 h.
525 In figure 8, data are expressed as dimensionless residual volume (i.e. volume at time *t*,
526 *V(t)*, divided by initial volume, V_0) of the selected organogels (OS70, OS80 and OS90),
527 at different time points. It is worth noticing that, assuming an approximately spherical
528 geometry, it holds:

529
$$\left(\frac{V(t)}{V_0}\right)=\left(\frac{M(t)}{M_0}\right)=\left(\frac{R(t)}{R_0}\right)^3 \qquad (8)$$

530 where *M* is the volume of organogel sample and *R* is the radius of the sphere, subscript
531 "0" refers to initial condition (i.e. at time t=0).

532 The volume profile as a function of time can be divided into two phases: phase I, up to
533 approximately 120 min, corresponding to the gastric step, in which material erosion is
534 fast, and phase II, from 120 on, in which the process slows down. At the end of the
535 tests, all the samples lost around 40% of their initial volume. It is worth noticing that,
536 owing to experimental difficulties, the error, for each point, is very large and this makes

537 the differences among tested samples insignificant. Anyway, if only the mean values are
538 considered, it can be seen that organogels with higher amounts of GMP, more
539 consistent, showed a reduced percentage of mass loss, with respect to those with higher
540 amounts of GMS. In particular, the highest difference can be observed by comparison of
541 OS90 and OS80 to OS70.

542 According to the literature [58] different models, mainly based on experimental data, were
543 proposed to describe the matrix erosion, among them the so-called "root type model"
544 seems able to fit a wide range of experimental results:

545 $$\frac{V(t)}{V_0} = \left(\frac{R(t)}{R_0}\right)^3 = 1 - (k_0 t)^a \quad (9)$$

546 where k_0 is the erosion rate constant and a is a fitting parameter. This model was used to
547 fit experimental values, evidencing a very good agreement (see Fig. 7) and obtained
548 parameters are reported in table 2.

549 Release kinetic can be modelled describing the mass transport between the carrier and
550 the surrounding fluid. If it is assumed that the main mechanism involved in drug release
551 is matrix erosion and, therefore, neglecting potential concentration profiles within the
552 carrier, it can be written:

553 $$\frac{dM_d(t)}{dt} = N_d A \quad (10)$$

554 where $M_d(t)$ is the drug mass within the carrier at each time t, A is the carrier external
555 surface, and N_d is the drug flux from the carrier towards the fluid; this can be described

556 in terms of a transport coefficient k_c and a driving force that is given by the
557 concentration difference in the liquid phase [59]:

558 $$N_d = -k_c\left(c_s - c(t)\right) \quad (11)$$

559 where *c(t)* is the drug mass concentration in the surrounding fluid at time t and c_s the
560 drug equilibrium solubility at the experimental temperature [53].

561 Assuming that the drug concentration in the liquid, *c(t),* is much lower than the
562 solubility limit (i.e. working under "sink" conditions, [53]) it can be neglected with respect
563 to c_s and eq. 11 becomes

564 $$\frac{dM_d(t)}{dt} = -k_c A c_s = -k_2 A \quad (12)$$

565 Where the solubility limit, being constant, has been included in k_2 that represents, in the
566 present case, a specific release rate with a meaning similar to that of the Korsmeyer-
567 Peppas constant k_1.

568 It is worth noticing that, when matrix erosion occurs, the external surface area is not
569 constant with time, therefore its change with time should be properly described to take
570 into account the effects on drug release. If eq. 9 is used to describe the volume evolution
571 and a spherical geometry is assumed, the evolution of external surface can be described
572 as:

573 $$\frac{A(t)}{A_0} = \left(\frac{R(t)}{R_0}\right)^2 = \left(1 - (k_0 t)^a\right)^{\frac{2}{3}} \quad (13)$$

574 where A_0 is the external surface at time 0. By replacing eq. 13 in eq. 12, it holds:

$$\frac{dM_d(t)}{dt} = -k_2 A(t) = -k_2\left(4\pi R_0^2\right)\left(1-\left(k_0 t\right)^a\right)^{\frac{2}{3}} \quad (14)$$

This equation can be solved using the initial condition t=0, $M_d(t)=M_{d0}$ obtaining:

$$1-\frac{M_d(t)}{M_{d0}} = F(t) = \frac{k_2}{M_{d0}}\left(4\pi R_0^2\right)\int_0^t\left(1-\left(k_0 t\right)^a\right)^{\frac{2}{3}} dt \quad (15)$$

The constant k_2 can be estimated following the procedure commonly adopted in chemical kinetic analysis and based on the integral method of data analysis [60]: eq. 15 is adopted to describe experimental data at time t= 2 h and t= 6 h, obtaining two values for the missing kinetic constant. If the suggested model is suitable to describe experimental data, the obtained values of kinetic constants are very similar each to the other (within the experimental error) and their mean value can be assumed as k_2 [60].

Obtained parameters for samples FOS70, FOS80 and FOS90 are shown in Table 3, in terms of mean value and standard deviation, it can be seen that, except for sample FOS80, deviation is very low (lower than 10%), within the expected experimental error, suggesting that the model is able to describe the data and therefore confirming the validity of the assumptions used. Table 3 reports the values of k_1 and n for the same samples: for all samples a value of n ranging between 0.43 and 0.85 was found, evidencing a potential anomalous diffusion mechanism.

Figure 9 shows the delivery data in terms of $F(t)$ with time for samples FOS70, FOS80 and FOS90; in addition the fitting curves of the Korsmeyer–Peppas model (eq. 6) and erosion model (eq. 15) are reported.

It is worth noticing that deviation between erosion model (eq. 15) and experimental data is approximately 5% for samples FOS70 and FOS90 whereas it is 14% for FOS80; this suggests that the model, although very simple, is able to describe experimental data strengthening the hypothesis of erosion controlled release. Moreover, it has a greater physical meaning than empirical fittings because it is based on a (simplified) physical description of observed phenomena and could be improved further removing some simplifying hypotheses.

The Korsmeyer–Peppas model, being a fitting equation with two adjustable parameters, describes almost perfectly the experimental data; nevertheless, it seems less related to the physical phenomena involved in the process.

Further tests, where a larger number of data are collected, seem necessary to discriminate better between different mechanisms evidencing the potential need to introduce a diffusion term in the mass balance equation.

4. CONCLUSIONS

This paper describes the thermo-rheological properties and the drug release characteristics of oleogels based on virgin olive oil and a mixture of glycerol monopalmitate (GMP) and glycerol monostearate (GMS). These low molecular weight organogelators are adopted in different areas, nevertheless they are commonly used in commercial mixtures, and therefore, few data are available on the effects of their ratio on macroscopic properties of obtained organogels.

615 A deep rheological investigation, based on dynamic and steady tests, evidenced that
616 GMP is more efficient than GMS in organogel production, making more consistent gels
617 with lower crystallization and gelation temperatures. These macroscopic differences can
618 be attributed to different microstructures, according to the results of rheo-optical and IR
619 characterisation. In fact, it was observed that, increasing GMS content, the crystalline
620 shape changes from a fiber-like structure to spherical clusters. Moreover, when the two
621 peaks associated with H bonding in infrared spectra are considered, the ratio between
622 peak heights and the peak intensities are a function of the GMS/GMP ratio and the
623 observed trend suggests the presence of fewer interactions with increasing amount of
624 GMS.

625 These results can be extremely useful in tuning organogel properties as a function of the
626 specific use; in the present work, they were used to develop a potential carrier for
627 controlled drug delivery, using 5 fluorouracil (5-FU) as the molecule to be released.
628 Experimental *in vitro* tests, evidenced, as expected, that organogels can yield a
629 controlled and progressive release of the drug, with respect to the unstructured oil.
630 Among tested samples the organogel containing 90% of GMS (over the total MAGs
631 content) seems the most promising because it yields a total release of approximately
632 40% of total loaded drug, with the largest fraction released in the intestinal tract.
633 Nevertheless, the formulation should be investigated further to enhance the total
634 released amount (currently quite low).

635 Drug release data has been described by a very simple physical model based on carrier
636 erosion that has proven itself to fit experimental value very well (the largest deviation
637 was 14%); this seems to confirm (according also to other literature works) that erosion
638 is the most important mechanism involved in drug release from organogels.

639

640 **5. AKNOWLEDGMENTS**

641 The authors are grateful to Dr Roberta Bianco for carrying out in-flow tests.

642

643 **REFERENCES**

644

645 1. C. L. Esposito, P. Kirilov and V. G. Roullin, Organogels, promising drug
646 delivery systems: an update of state-of-the-art and recent applications, *Journal of*
647 *Controlled Release*, 2018, **271**, 1-20.

648 2. Q. Zhang, Y. M. Song, S. W. Page and S. Garg, Evaluation of Transdermal Drug
649 Permeation as Modulated by Lipoderm and Pluronic Lecithin Organogel, *Journal of*
650 *Pharmaceutical Sciences*, 2018, **107**, 587-594.

651 3. Z. L. Li, B. Zhang, S. H. Jia, M. F. Ma and J. C. Hao, Novel supramolecular
652 organogel based on beta-cyclodextrin as a green drug carrier for enhancing anticancer
653 effects, *Journal of Molecular Liquids*, 2018, **250**, 19-25.

654 4. D. E. Liu, Q. X. Chen, Y. B. Long, J. B. Ma and H. Gao, A thermo-responsive
655 polyurethane organogel for norfloxacin delivery, *Polymer Chemistry*, 2018, **9**, 228-235.

656 5. S. P. Kodela, P. M. Pandey, S. K. Nayak, K. Uvanesh, A. Anis and K. Pal,
657 Novel agar-stearyl alcohol oleogel-based bigels as structured delivery vehicles,
658 *International Journal of Polymeric Materials and Polymeric Biomaterials*, 2017, **66**,
659 669-678.

660 6. A. Shakeel, F. R. Lupi, D. Gabriele, N. Baldino and B. De Cindio, Bigels: A
661 unique class of materials for drug delivery applications, *Soft Materials*, 2018, 1-17.

662 7. A. R. Patel, in *Edible Oil Structuring: Concepts, Methods and Applications*, The
663 Royal Society of Chemistry, 2018, pp. 1-22.

664 8. E. D. Co and A. G. Marangoni, Organogels: An Alternative Edible Oil-
665 Structuring Method, *Journal of the American Oil Chemists Society*, 2012, **89**, 749-780.

9. A. J. Martins, A. A. Vicente, R. L. Cunha and M. A. Cerqueira, Edible oleogels: an opportunity for fat replacement in foods, *Food & Function*, 2018, **9**, 758-773.

10. N. Siraj, M. A. Shabbir, T. Ahmad, A. Sajjad, M. R. Khan, M. I. Khan and M. S. Butt, Organogelators as a Saturated Fat Replacer for Structuring Edible Oils, *International Journal of Food Properties*, 2015, **18**, 1973-1989.

11. F. R. Lupi, D. Gabriele, N. Baldino, L. Seta, B. de Cindio and C. De Rose, Stabilization of meat suspensions by organogelation: A rheological approach, *European Journal of Lipid Science and Technolology*, 2012, **114**, 1381-1389.

12. D. J. McClements and H. Xiao, Excipient foods: designing food matrices that improve the oral bioavailability of pharmaceuticals and nutraceuticals, *Food & Function*, 2014, **5**, 1320-1333.

13. M. D. Bin Sintang, S. Danthine, A. Brown, D. Van de Walle, A. R. Patel, I. Tavernier, T. Rimaux and K. Dewettinck, Phytosterols-induced viscoelasticity of oleogels prepared by using monoglycerides, *Food Research International*, 2017, **100**, 832-840.

14. D. Kouzounis, A. Lazaridou and E. Katsanidis, Partial replacement of animal fat by oleogels structured with monoglycerides and phytosterols in frankfurter sausages, *Meat Science*, 2017, **130**, 38-46.

15. C. Palla, A. Giacomozzi, D. B. Genovese and M. E. Carrín, Multi–objective optimization of high oleic sunflower oil and monoglycerides oleogels: Searching for rheological and textural properties similar to margarine, *Food Structure*, 2017, **12**, 1-14.

16. M. D. B. Sintang, T. Rimaux, D. V. d. Walle, K. Dewettinck and A. R. Patel, Oil structuring properties of monoglycerides and phytosterols mixtures, *European Journal of Lipid Science and Technology*, 2017, **119**, 1500517.

17. H. Noureddini and V. Medikonduru, Glycerolysis of fats and methyl esters, *Journal of the American Oil Chemists' Society*, 1997, **74**, 419-425.

18. J. Blazek, E. P. Gilbert and L. Copeland, Effects of monoglycerides on pasting properties of wheat starch after repeated heating and cooling, *Journal of Cereal Science*, 2011, **54**, 151-159.

19. S. L. McSweeney, R. Healy and D. M. Mulvihill, Effect of lecithin and monoglycerides on the heat stability of a model infant formula emulsion, *Food Hydrocolloids*, 2008, **22**, 888-898.

20. E. Davies, E. Dickinson and R. Bee, Shear stability of sodium caseinate emulsions containing monoglyceride and triglyceride crystals, *Food Hydrocolloids*, 2000, **14**, 145-153.

21. R. Rafanan and D. Rousseau, Dispersed droplets as active fillers in fat-crystal network-stabilized water-in-oil emulsions, *Food Research International*, 2017, **99**, 355-362.

22. F. R. Lupi, M. P. De Santo, F. Ciuchi, N. Baldino and D. Gabriele, A rheological modelling and microscopic analysis of bigels, *Rheologica Acta*, 2017, **56**, 753-763.

23. F. R. Lupi, A. Shakeel, V. Greco, C. Oliviero Rossi, N. Baldino and D. Gabriele, A rheological and microstructural characterisation of bigels for cosmetic and pharmaceutical uses, *Materials Science and Engineering: C*, 2016, **69**, 358-365.

24. A. Alfutimie, N. Al-Janabi, R. Curtis and G. J. T. Tiddy, The Effect of monoglycerides on the crystallisation of triglyceride, *Colloids and Surfaces A: Physicochemical and Engineering Aspects*, 2016, **494**, 170-179.

25. A. Alfutimie, R. Curtis and G. J. T. Tiddy, Gel phase (Lβ) formation by mixed saturated and unsaturated monoglycerides, *Colloids and Surfaces A: Physicochemical and Engineering Aspects*, 2014, **456**, 286-295.

715 26. N. K. Ojijo, I. Neeman, S. Eger and E. Shimoni, Effects of monoglyceride
716 content, cooling rate and shear on the rheological properties of olive oil/monoglyceride
717 gel networks, *Journal of the Science of Food and Agriculture*, 2004, **84**, 1585-1593.

718 27. F. R. Lupi, A. Shakeel, V. Greco, N. Baldino, V. Calabrò and D. Gabriele,
719 Organogelation of extra virgin olive oil with fatty alcohols, glyceryl stearate and their
720 mixture, *LWT - Food Science and Technology*, 2017, **77**, 422-429.

721 28. F. R. Lupi, V. Greco, N. Baldino, B. de Cindio, P. Fischer and D. Gabriele, The
722 effects of intermolecular interactions on the physical properties of organogels in edible
723 oils, *Journal of Colloid and Interface Science*, 2016, **483**, 154-164.

724 29. F. R. Lupi, D. Gabriele, D. Facciolo, N. Baldino, L. Seta and B. de Cindio,
725 Effect of organogelator and fat source on rheological properties of olive oil-based
726 organogels, *Food Research International*, 2012, **46**, 177-184.

727 30. F. R. Lupi, D. Gabriele and B. de Cindio, Effect of Shear Rate on Crystallisation
728 Phenomena in Olive Oil-Based Organogels, *Food and Bioprocess Technology*, 2012, **5**,
729 2880-2888.

730 31. A. Lopez-Martinez, J. A. Morales-Rueda, E. Dibildox-Alvarado, M. A. Charo-
731 Alonso, A. G. Marangoni and J. F. Toro-Vazquez, Comparing the crystallization and
732 rheological behavior of organogels developed by pure and commercial monoglycerides
733 in vegetable oil, *Food Research International*, 2014, **64**, 946-957.

734 32. S. Da Pieve, S. Calligaris, E. Co, M. C. Nicoli and A. G. Marangoni, Shear
735 Nanostructuring of Monoglyceride Organogels, *Food Biophysics*, 2010, **5**, 211-217.

736 33. T. Pénzes, G. Blazsó, Z. Aigner, G. Falkay and I. Erős, Topical absorption of
737 piroxicam from organogels—in vitro and in vivo correlations, *International Journal of*
738 *Pharmaceutics*, 2005, **298**, 47-54.

34. T. Pénzes, I. Csóka and I. Erős, Rheological analysis of the structural properties effecting the percutaneous absorption and stability in pharmaceutical organogels, *Rheologica Acta*, 2004, **43**, 457-463.

35. R. Sanchez, J. M. Franco, M. A. Delgado, C. Valencia and C. Gallegos, Rheology of oleogels based on sorbitan and glyceryl monostearates and vegetable oils for lubricating applications, *Grasas Y Aceites*, 2011, **62**, 328-336.

36. A. Lopez-Martinez, M. A. Charo-Alonso, A. G. Marangoni and J. F. Toro-Vazquez, Monoglyceride organogels developed in vegetable oil with and without ethylcellulose, *Food Research International*, 2015, **72**, 37-46.

37. A. Vintiloiu and J.-C. Leroux, Organogels and their use in drug delivery — A review, *Journal of Controlled Release*, 2008, **125**, 179-192.

38. F. R. Lupi, D. Gabriele, N. Baldino, P. Mijovic, O. I. Parisi and F. Puoci, Olive oil/policosanol organogels for nutraceutical and drug delivery purposes, *Food & Function*, 2013, **4**, 1512-1520.

39. S. Uzan, D. Barış, M. Çolak, H. Aydın and H. Hoşgören, Organogels as novel carriers for dermal and topical drug delivery vehicles, *Tetrahedron*, 2016, **72**, 7517-7525.

40. A. Fallah Shojaei, K. Tabatabaeian, S. Shakeri and F. Karimi, A novel 5-fluorouracile anticancer drug sensor based on ZnFe2O4 magnetic nanoparticles ionic liquids carbon paste electrode, *Sensors and Actuators B: Chemical*, 2016, **230**, 607-614.

41. P. Singh, G. Tyagi, R. Mehrotra and A. K. Bakhshi, Thermal stability studies of 5-fluorouracil using diffuse reflectance infrared spectroscopy, *Drug Testing and Analysis*, 2009, **1**, 240-244.

762 42. K. Miura, M. Kinouchi, K. Ishida, W. Fujibuchi, T. Naitoh, H. Ogawa, T. Ando,
763 N. Yazaki, K. Watanabe, S. Haneda, C. Shibata and I. Sasaki, 5-FU Metabolism in
764 Cancer and Orally-Administrable 5-FU Drugs, *Cancers*, 2010, **2**, 1717.

765 43. F. R. Lupi, D. Gabriele, V. Greco, N. Baldino, L. Seta and B. de Cindio, A
766 rheological characterisation of an olive oil/fatty alcohols organogel, *Food Research*
767 *International*, 2013, **51**, 510-517.

768 44. J. H. van Esch and B. L. Feringa, New Functional Materials Based on Self-
769 Assembling Organogels: From Serendipity towards Design, *Angewandte Chemie*
770 *International Edition*, 2000, **39**, 2263-2266.

771 45. S. Wu, J. Gao, T. J. Emge and M. A. Rogers, Influence of solvent on the
772 supramolecular architectures in molecular gels, *Soft Matter*, 2013, **9**, 5942-5950.

773 46. C. H. Chen and E. M. Terentjev, Aging and Metastability of Monoglycerides in
774 Hydrophobic Solutions, *Langmuir*, 2009, **25**, 6717-6724.

775 47. M. Suzuki, T. Abe and K. Hanabusa, Low-molecular-weight gelators based on
776 N-alpha-acetyl-N-epsilon-dodecyl-L-lysine and their amphiphilic gelation properties,
777 *Journal of Colloid and Interface Science*, 2010, **341**, 69-74.

778 48. S. Shin, J. Jang, S. H. Yoon and I. Mochida, A study on the effect of heat
779 treatment on functional groups of pitch based activated carbon fiber using FTIR,
780 *Carbon*, 1997, **35**, 1739-1743.

781 49. D. Tang and A. G. Marangoni, Modified fractal model and rheological
782 properties of colloidal networks, *Journal of Colloid and Interface Science*, 2008, **318**,
783 202-209.

784 50. H.-S. Hwang, S. Kim, K. O. Evans, C. Koga and Y. Lee, Morphology and
785 networks of sunflower wax crystals in soybean oil organogel, *Food Structure*, 2015, **5**,
786 10-20.

787 51. B. Crist and J. M. Schultz, Polymer spherulites: A critical review, *Progress in*
788 *Polymer Science*, 2016, **56**, 1-63.

789 52. R. Kumar, S. Patil, M. B. Patil, S. R. Patil and M. S. Paschapur, Design and In
790 vitro Evaluation of Oral Floating Matrix Tablets of Aceclofenac, *International Journal*
791 *of ChemTech Research*, 2009, **1**, 10.

792 53. S. N. Raza and N. A. Khan, Role of mathematical modelling in controlled
793 release drug delivery, *International Journal of Medical Research and Pharmaceutical*
794 *Sciences*, 2017, **4**, 84-95.

795 54. U. R. Pothakamury and G. V. Barbosa-Cánovas, Fundamental aspects of
796 controlled release in foods, *Trends in Food Science & Technology*, 1995, **6**, 397-406.

797 55. R. W. Korsmeyer, R. Gurny, E. Doelker, P. Buri and N. A. Peppas, Mechanisms
798 of solute release from porous hydrophilic polymers, *International Journal of*
799 *Pharmaceutics*, 1983, **15**, 25-35.

800 56. K. Iwanaga, T. Sumizawa, M. Miyazaki and M. Kakemi, Characterization of
801 organogel as a novel oral controlled release formulation for lipophilic compounds, *Int J*
802 *Pharm*, 2010, **388**, 123-128.

803 57. J. Siepmann and F. Siepmann, Mathematical modeling of drug delivery,
804 *International Journal of Pharmaceutics*, 2008, **364**, 328-343.

805 58. S. You, Z. Yang and C.-H. Wang, Toward Understanding Drug Release From
806 Biodegradable Polymer Microspheres of Different Erosion Kinetics Modes, *Journal of*
807 *Pharmaceutical Sciences*, 2016, **105**, 1934-1946.

808 59. R. B. Bird, W. E. Stewart and E. N. Lightfoot, *Transport Phenomena*, John
809 Wiley and sons, Inc., USA, 2nd edn., 2007.

60. J. M. Smith, *Chemical Engineering Kinetics*, McGraw-Hill International Edition, 3rd edn., 1981.

814 **TABLES CAPTIONS**

815

816 Table 1 Samples ID and composition; onset of crystallisation temperature, Tco, at
817 1 and 10 s^{-1} are calculated by SRTRTs; the ratio 5FU/oil is constant and equal to 0.016.

818 Table 2 Fitting parameters of eq. 6 applied to experimental data of samples OS70,
819 OS80, OS90

820 Table 3 Korsmeyer-Peppas model parameters (k_1 and n, eq. 6) and erosion model
821 parameter (k_2, eq. 15) for samples FOS70, FOS80, FOS90.

822

FIGURES CAPTIONS

Figure 1 Schematic representation of organogels and their uses: organogelator molecules aggregate into crystals and clusters creating the organogel. In turn, different other fillers can differentiate among the possible uses of organogels

Figure 2 Dynamic temperature ramp tests of samples OS50 (red diamond), OS60 (blue square), OS70 (open circle), OS80 (green circle), OS90 (purple triangle), OS100 (brown cross). Complex modulus G* (a) and phase angle δ (b).

Figure 3 ΔTco vs x_{GMS}=GMS/MAGs; ΔTco is calculated according to eq. (1)

Figure 4 Rheological parameters at T=20°C for different glycerol monostearate fraction, X_{GMS}. (a) Viscosity, η, calculated at $1s^{-1}$ (solid circles) and 10 s^{-1} (open circles); (b) complex modulus, G*, (solid circles) and phase angle, δ, (open circles).

Figure 5 Infrared spectra of organogels (a) and storage modulus, G', at 20°C versus A_{OH}, experimental data (symbols) and modified fractal model (eq. 4) (b)

Figure 6 Micrographs of samples OS50, OS70 and OS100 taken with the rheoscope tool during temperature ramp tests in dynamic (SAOT) and steady (SRTRT) conditions. Reference bar is 50 μm.

Figure 7 Fraction of 5-FU released in each tract (the "gastric" and the "intestinal" tract) with respect to initial drug mass. Gastric phase refers to the *in vitro* step simulating the gastric tract; intestinal phase refers to the *in vitro* step simulating the intestinal tract.

Figure 8 Dimensionless volume profile with time of organogels capsules OS70 (circle), OS80 (diamond) and OS90 (square). For each sample, fitting lines refers to eq. 6. V(t) is the capsule volume at the time t, V_0 is the initial capsule volume.

Figure 9 Delivery data in terms of F(t) with time for samples FOS70 (circle), FOS80 (diamond) and FOS90 (square); the fitting curves of the Korsmeyer–Peppas model (eq. 7, solid line) and erosion model (eq. 13, dashed line) are shown.

849

Sample	Olive oil (%w/w)	GMP (%w/w)	GMS (%w/w)	5-FU (%w/w)	x_{GMS} (w/w)	Tco 1 s^{-1} (°C)	Tco 10 s^{-1} (°C)	Tco SAOTs (°C)	Tg (°C)
OS50	95	2.5	2.5	-	0.50	49.2±0.1	48.2±0.3	50.8±0.2	48.1±0.1
OS60	95	2	3	-	0.60	48.4±0.6	45.8±0.3	48.7±0.3	46.3±0.3
OS70	95	1.5	3.5	-	0.70	47.0±0.3	43.0±0.3	46.8±0.3	44.1±0.1
OS80	95	1	4	-	0.80	42.0±0.1	37.8±0.3	42.5±0.1	40.9±0.2
OS90	95	0.5	4.5	-	0.90	39.4±0.3	35.2±0.1	40.8±0.2	38.6±0.1
OS100	95	-	5	-	1.00	33.6±0.1	29.2±0.1	33.2±0.4	31.6±0.4
FOS70	93.5	1.5	3.5	1.5	0.70	-	-	-	-
FOS80	93.5	1	4	1.5	0.80	-	-	-	-
FOS90	93.5	1.5	4.5	1.5	0.90	-	-	-	-
FO	98.42	-	-	1.58	-	-	-	-	-

850

851 Table 1

Sample	k_0 (-)	a (-)
OS70	$(1.59\pm 0.16)\ 10^{-5}$	0.430 ± 0.030
OS80	$(6.10\pm 0.78)\ 10^{-6}$	0.364 ± 0.017
OS90	$(6.00\pm 0.70)\ 10^{-6}$	0.404 ± 0.018

852

853 Table 2

854

Sample	k_1 (s^{-n})	n (-)	k_2 ($kg/s/m^2$)
FOS70	$(9.18\pm 0.01)\cdot 10^{-5}$	0.760 ± 0.001	$(4.2\pm0.2)\cdot 10^{-3}$
FOS80	$(2.98 \pm 0.01)\cdot 10^{-4}$	0.680 ± 0.001	$(6\pm1)\cdot 10^{-3}$
FOS90	$(1.02 \pm 0.01)\cdot 10^{-4}$	0.818 ± 0.001	$(7.2\pm0.5)\cdot 10^{-3}$

855

856 Table 3

857

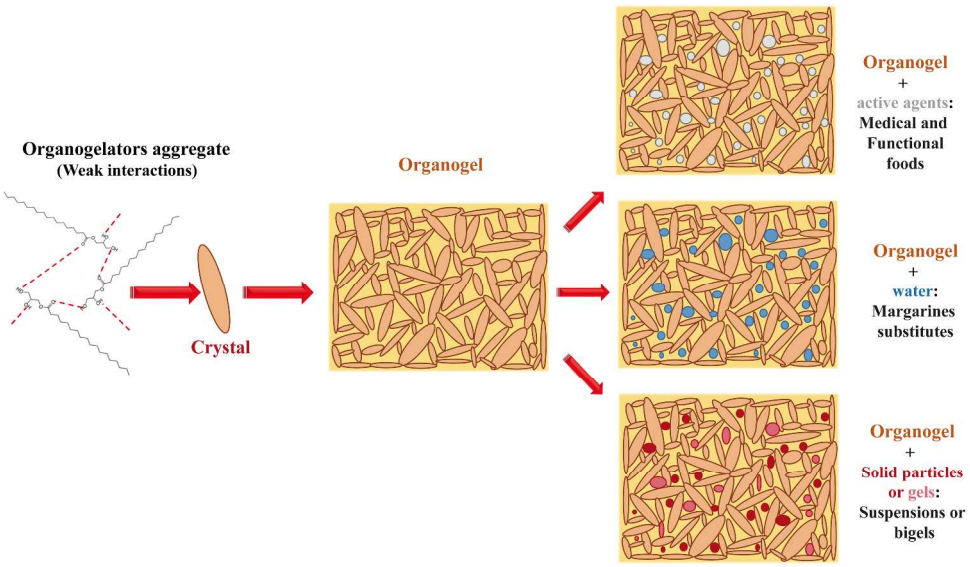

Figure 1 Schematic representation of organogels and their uses: organogelator molecules aggregate into crystals and clusters creating the organogel. In turn, different other fillers can differentiate among the possible uses of organogels

297x167mm (300 x 300 DPI)

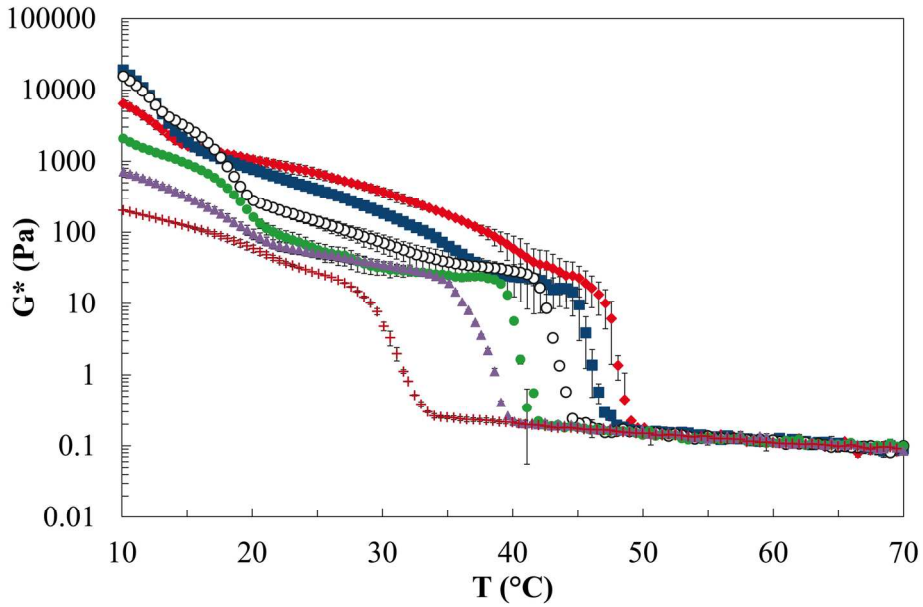

Figure 2 Dynamic temperature ramp tests of samples OS50 (red diamond), OS60 (blue square), OS70 (open circle), OS80 (green circle), OS90 (purple triangle), OS100 (brown cross). Complex modulus G* (a) and phase angle δ (b).

173x108mm (300 x 300 DPI)

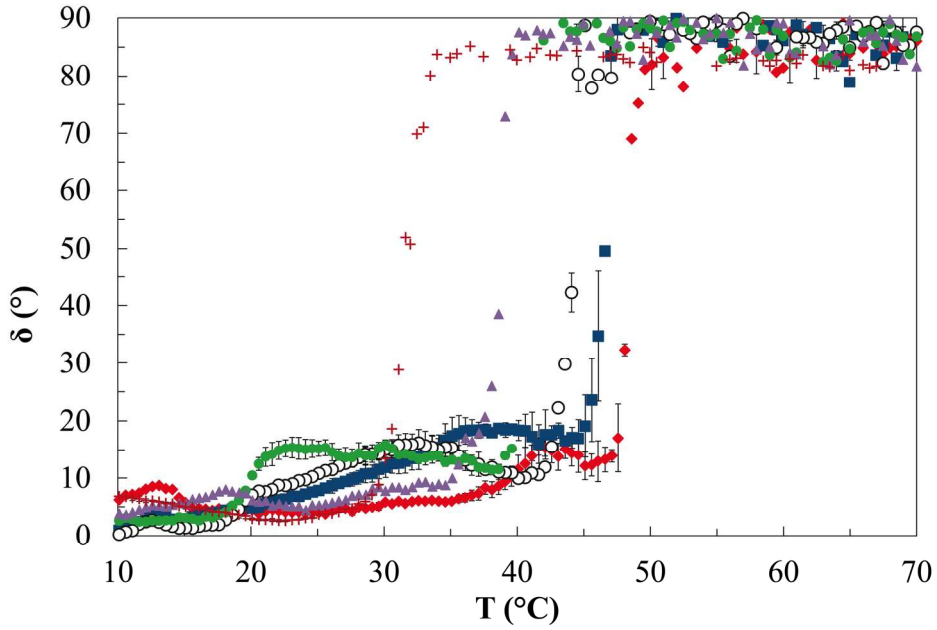

Figure 2 Dynamic temperature ramp tests of samples OS50 (red diamond), OS60 (blue square), OS70 (open circle), OS80 (green circle), OS90 (purple triangle), OS100 (brown cross). Complex modulus G* (a) and phase angle δ (b).

173x112mm (300 x 300 DPI)

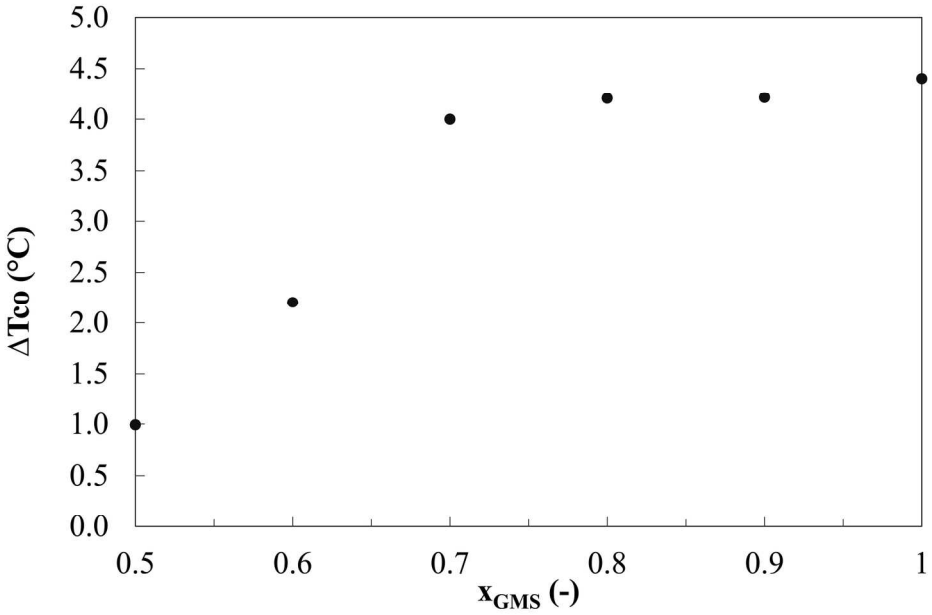

Figure 3 ΔTco vs xGMS=GMS/MAGs; ΔTco is calculated according to eq. (1)

170x107mm (300 x 300 DPI)

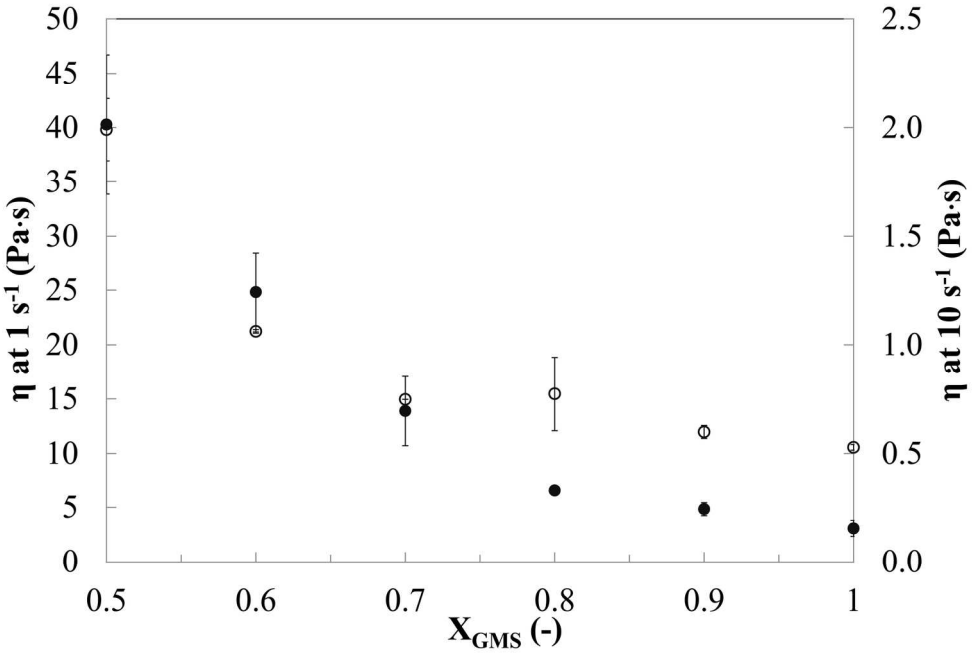

Figure 4 Rheological parameters at T=20°C for different glycerol monostearate fraction, XGMS. (a) Viscosity, η, calculated at 1s-1 (solid circles) and 10 s-1 (open circles); (b) complex modulus, G*, (solid circles) and phase angle, δ, (open circles).

172x115mm (300 x 300 DPI)

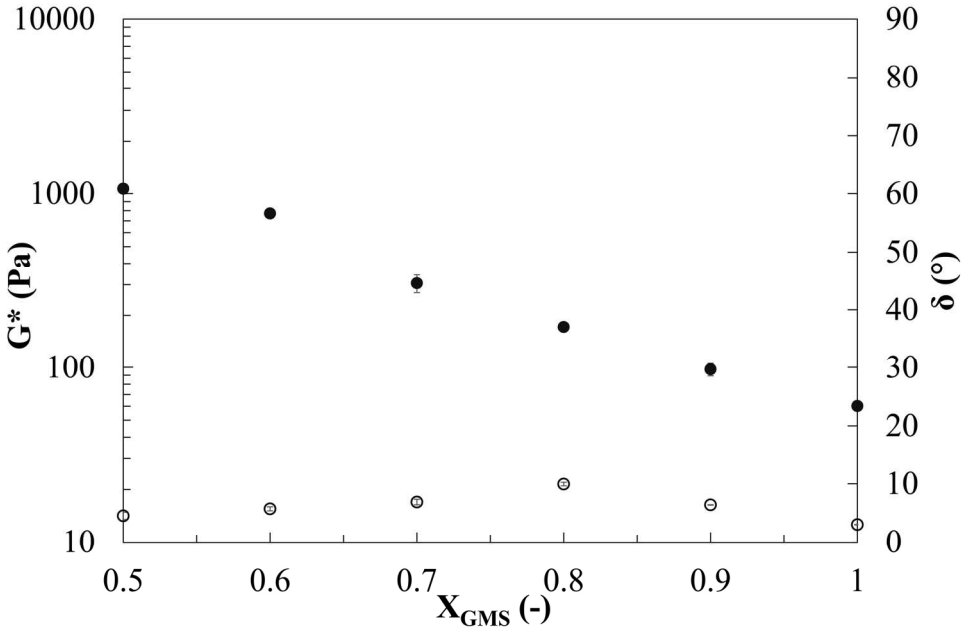

Figure 4 Rheological parameters at T=20°C for different glycerol monostearate fraction, XGMS. (a) Viscosity, η, calculated at 1s-1 (solid circles) and 10 s-1 (open circles); (b) complex modulus, G*, (solid circles) and phase angle, δ, (open circles).

166x108mm (300 x 300 DPI)

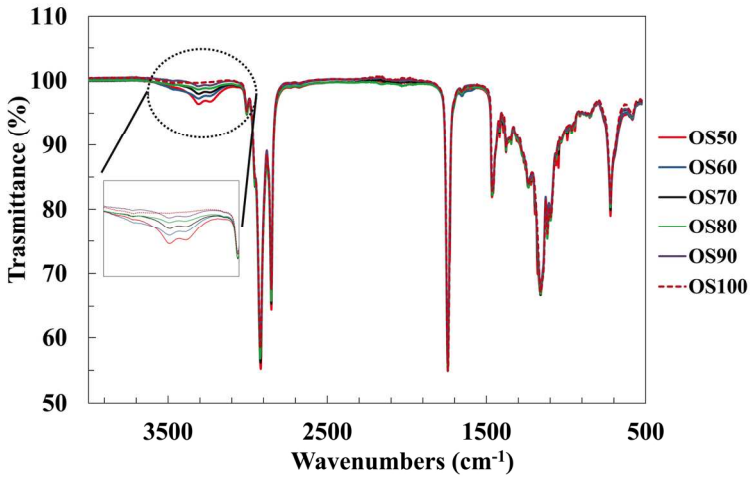

Figure 5 Infrared spectra of organogels (a) and storage modulus, G', at 20°C versus AOH, experimental data (symbols) and modified fractal model (eq. 4) (b)

167x93mm (300 x 300 DPI)

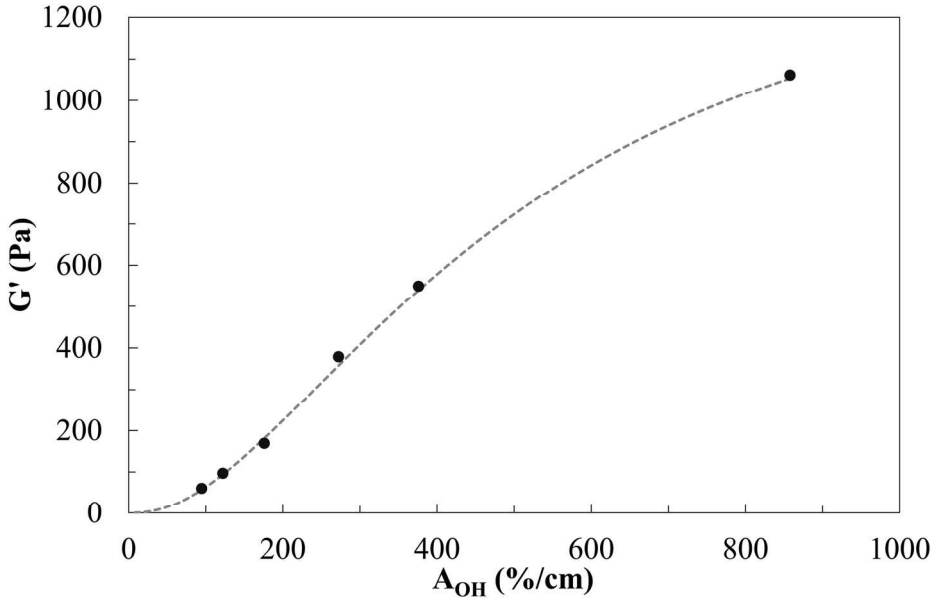

Figure 5 Infrared spectra of organogels (a) and storage modulus, G', at 20°C versus AOH, experimental data (symbols) and modified fractal model (eq. 4) (b)

169x104mm (300 x 300 DPI)

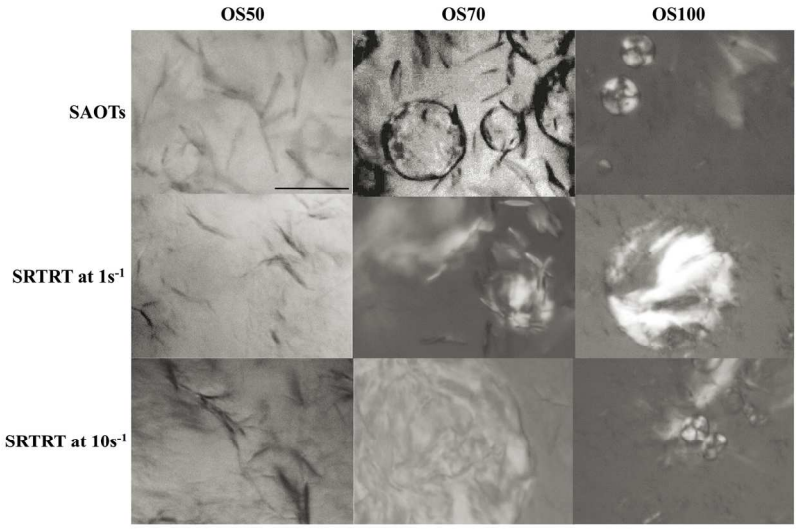

Figure 6 Micrographs of samples OS50, OS70 and OS100 taken with the rheoscope tool during temperature ramp tests in dynamic (SAOT) and steady (SRTRT) conditions. Reference bar is 50 μm.

167x93mm (300 x 300 DPI)

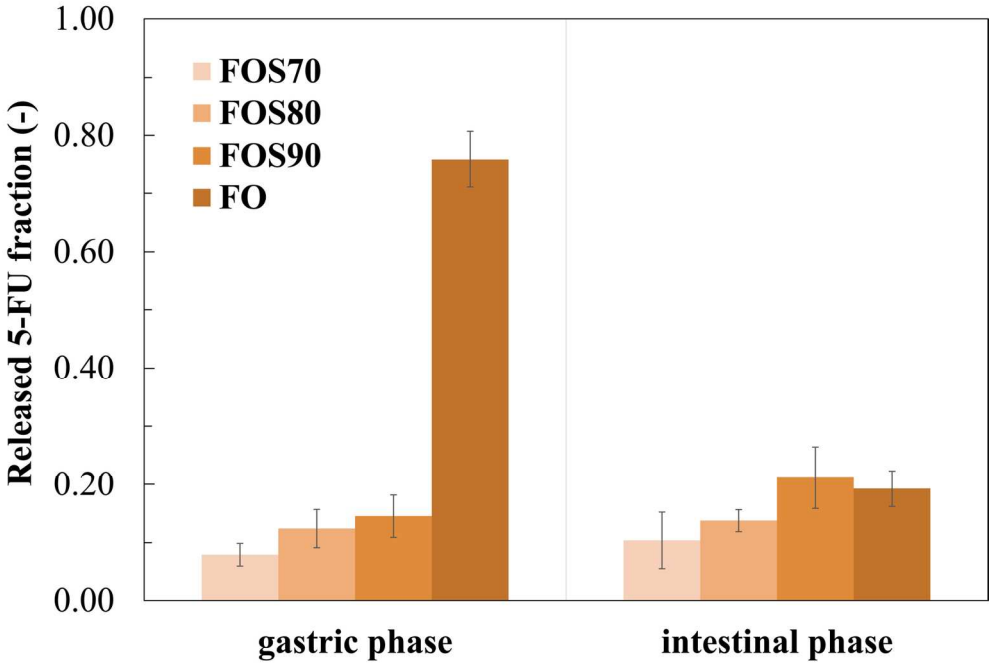

Figure 7 Fraction of 5-FU released in each tract (the "gastric" and the "intestinal" tract) with respect to initial drug mass. Gastric phase refers to the in vitro step simulating the gastric tract; intestinal phase refers to the in vitro step simulating the intestinal tract.

166x113mm (300 x 300 DPI)

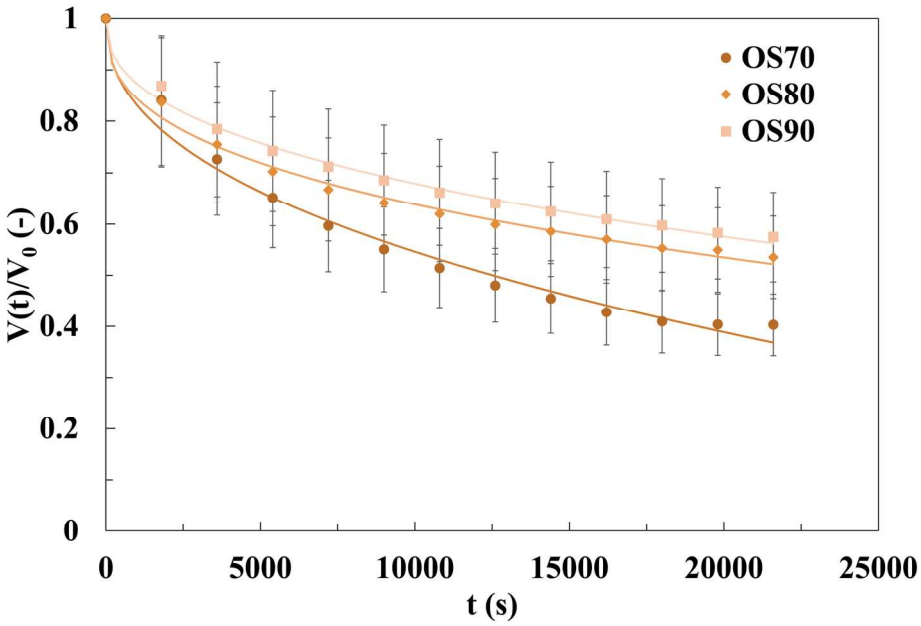

Figure 8 Dimensionless volume profile with time of organogels capsules OS70 (circle), OS80 (diamond) and OS90 (square). For each sample, fitting lines refers to eq. 6. V(t) is the capsule volume at the time t, V0 is the initial capsule volume.

172x110mm (300 x 300 DPI)

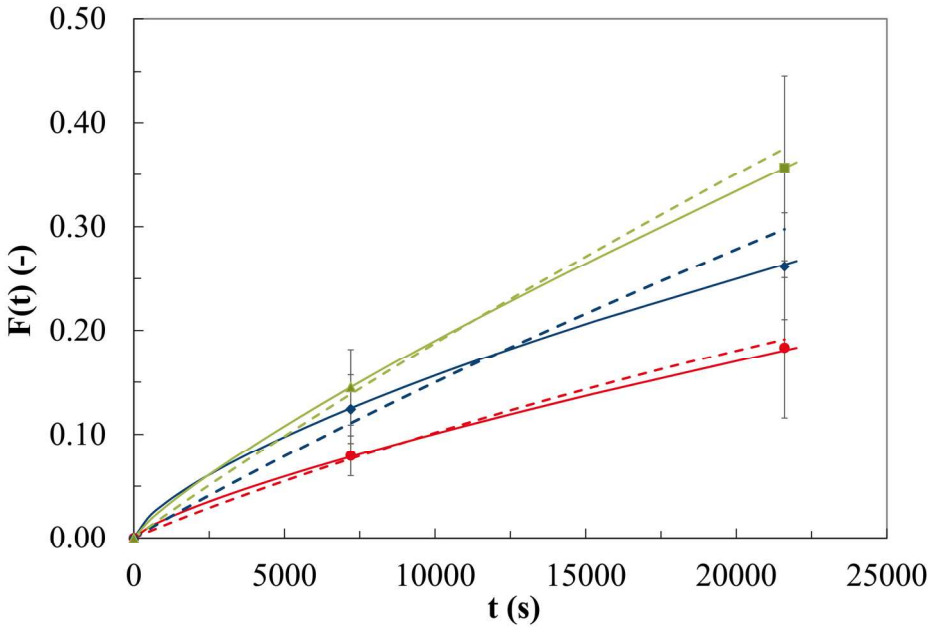

Figure 9 Delivery data in terms of F(t) with time for samples FOS70 (circle), FOS80 (diamond) and FOS90 (square); the fitting curves of the Korsmeyer–Peppas model (eq. 7, solid line) and erosion model (eq. 13, dashed line) are shown.

168x109mm (300 x 300 DPI)

GMP/GMS organogels are promising systems for oral delivery in functional or medical foods

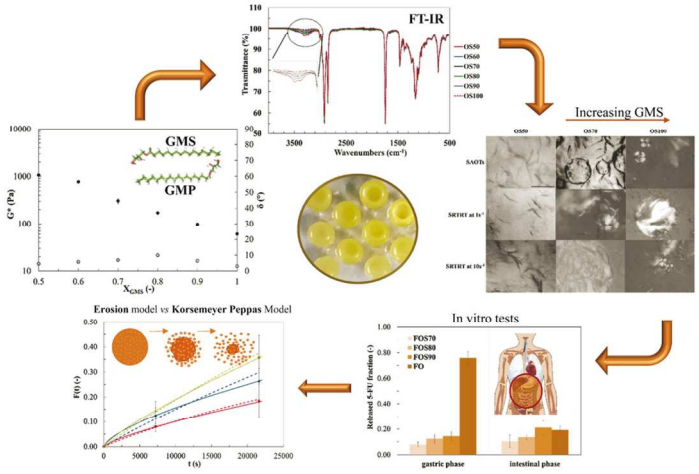

123x82mm (300 x 300 DPI)

Effect of the monostearate/monopalmitate ratio on oral release of active agents from monoacylglycerols organogels

F. R. Lupi[1], V. Mancina[1], N. Baldino[1], O.I. Parisi[2], L. Scrivano[2], D. Gabriele[1]

[1] Department of Information, Modelling, Electronics and System Engineering, (D.I.M.E.S.) University of Calabria, Via P. Bucci, Cubo 39C, I-87036 Rende (CS), Italy

francesca.lupi@unical.it; mancina.valentina@gmail.com; noemi.baldino@unical.it; domenico.gabriele@unical.it; ortensiailaria.parisi@unical.it; luca.scrivano@unical.it

[2] Department of Pharmacy, Health and Nutritional Sciences, University of Calabria, Edificio Polifunzionale, I-87036 Rende (CS), Italy

Corresponding author
Dr. Domenico Gabriele
Email: domenico.gabriele@unical.it

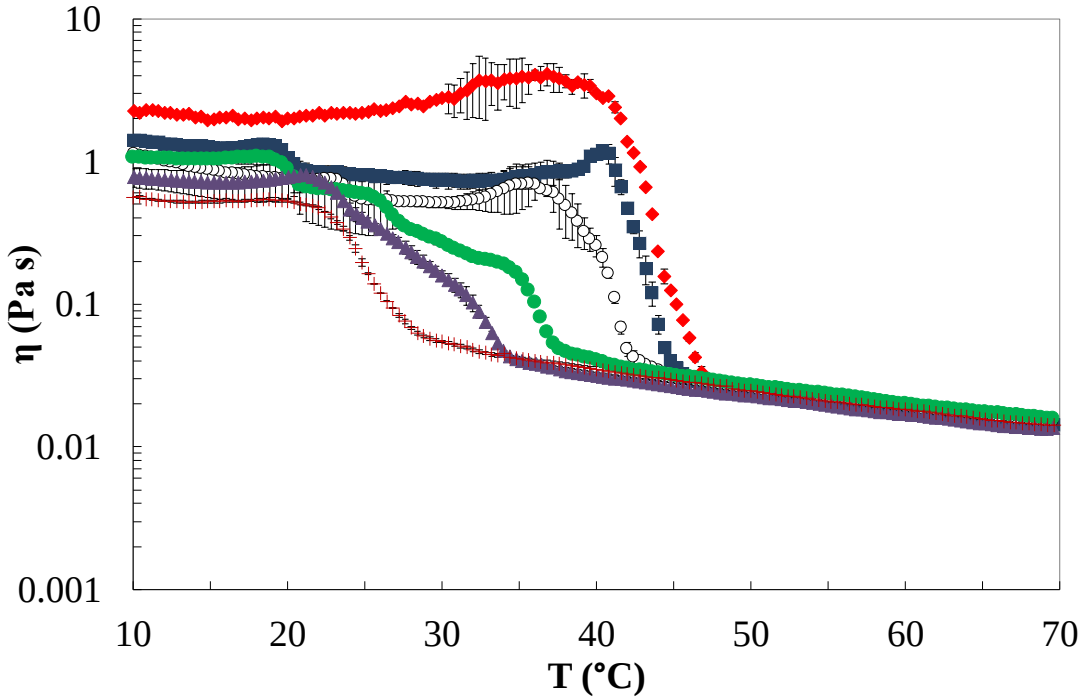

Figure SM1 Steady temperature ramp tests at 1 s^{-1} of samples OS50 (red diamond), OS60 (blue square), OS70 (open circle), OS80 (green circle), OS90 (purple triangle), OS100 (brown cross).

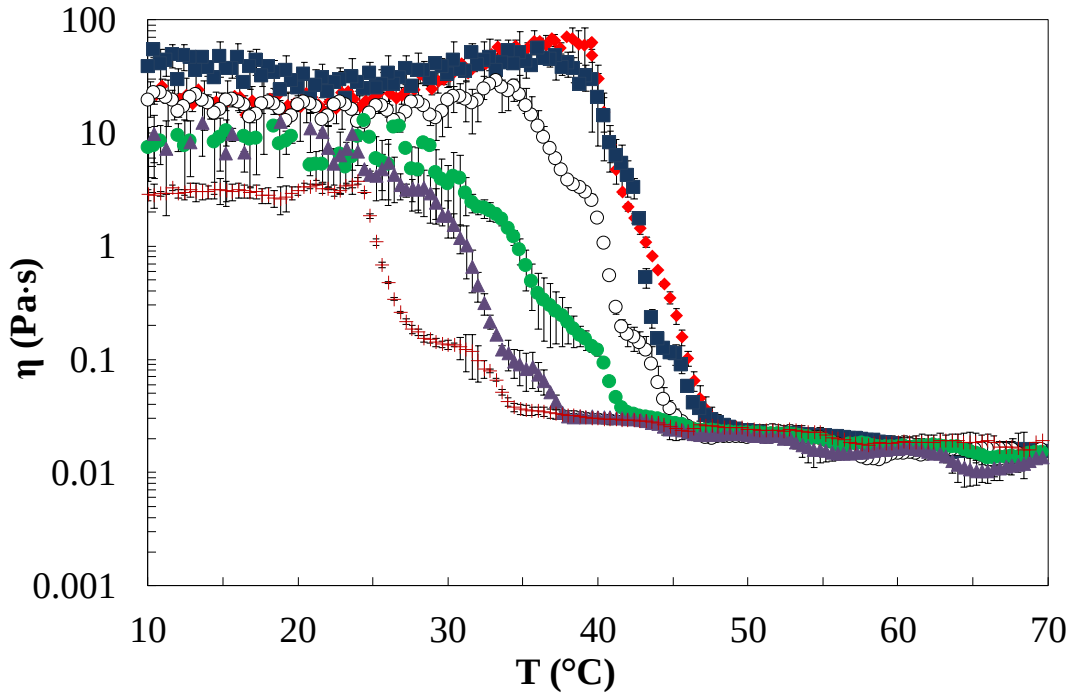

Figure SM2 Steady temperature ramp tests at 10 s^{-1} of samples OS50 (red diamond), OS60 (blue square), OS70 (open circle), OS80 (green circle), OS90 (purple triangle), OS100 (brown cross).

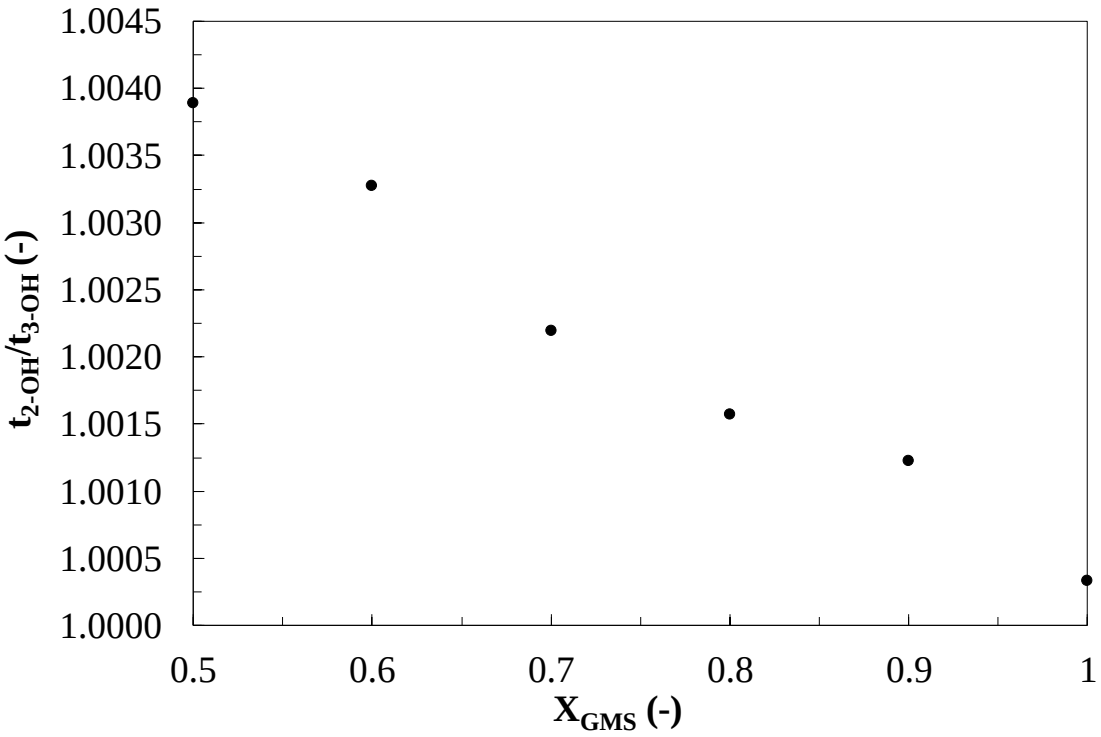

Figure SM3 Ratio between transmittance value of peak 2-OH over peak 3-OH ($t_{2\text{-}OH}/t_{3\text{-}OH}$) versus X_{GMS}